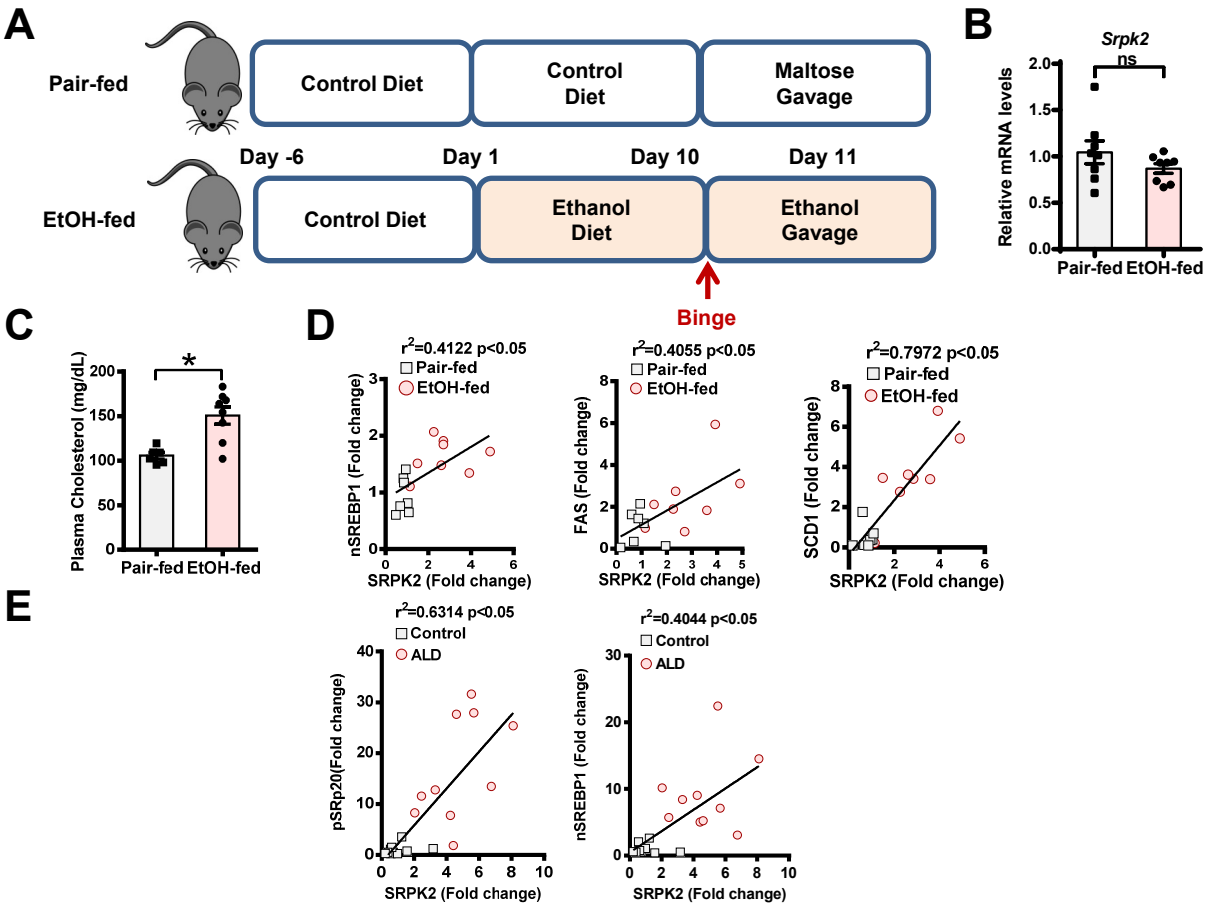

Fig. S1. Illustration of a pre-clinical mouse model of chronic-plus-binge alcohol feeding-induced hepatic steatosis and liver injury, related to Fig. 1.

A. The schematic illustration of a chronic-plus-binge alcohol feeding mouse model. C57BL/6 mice were subjected to a Lieber-DeCarli alcohol liquid diet for 10 days, followed by one binge alcohol feeding at the end of experiments, while the control group received a pair-fed control liquid diet. A control liquid diet and an alcohol liquid diet were isocaloric. All mice were sacrificed 9 hours post-binge.

B. Real-time quantitative RT-PCR analysis of mRNA levels of SRPK2 in the livers of mice described in **A.**

C. Plasma cholesterol levels in pair-fed and ethanol-fed mice. The data are presented as the mean ± S.E.M., n=6-8 per group. *P<0.05, vs pair-fed mice.

D. Correlation between hepatic levels of SRPK2 protein and those of nSREBP-1, FAS, and SCD1 in pair-fed and alcohol-fed mice.

E. Correlation between hepatic levels of SRPK2 and those of SR protein phosphorylation and nSREBP-1 in healthy human controls and ALD patients.

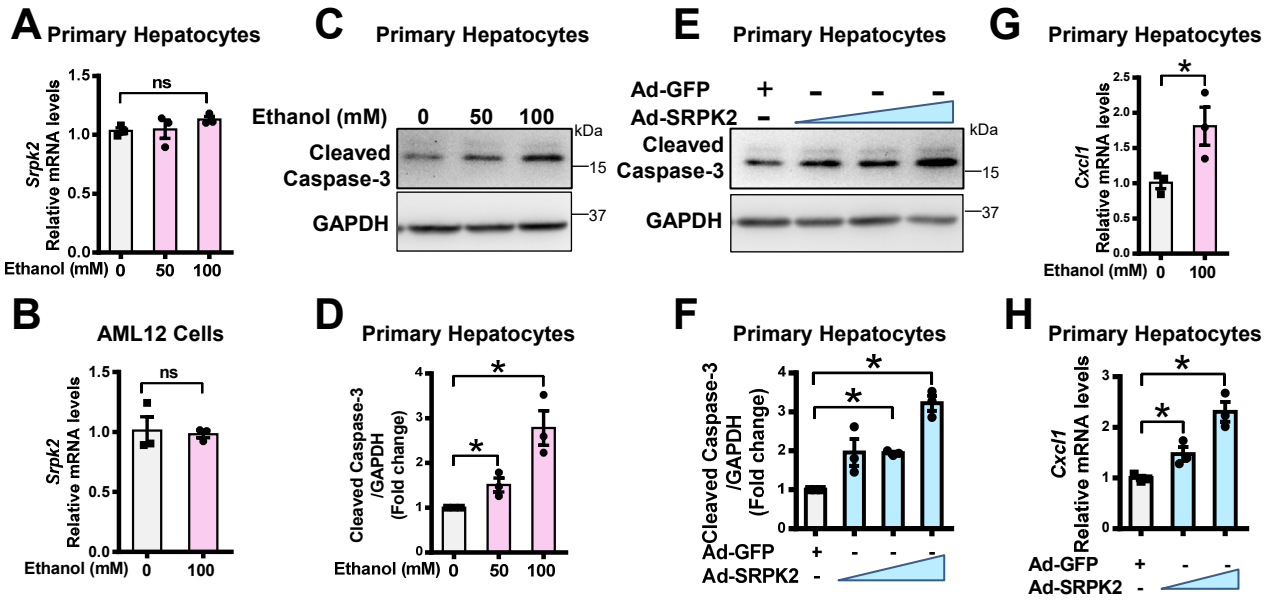

Fig. S2. Adenovirus-mediated overexpression of SRPK2 mimics the ability of ethanol to induce cell apoptosis and the production of the inflammatory mediator CXCL1 in primary mouse hepatocytes, related to Fig. 2 and 3.

A-B. Real-time qRT-PCR revealed no significant changes in SRPK2 mRNA when protein levels were increased in ethanol-treated primary mouse hepatocytes (**A**) or AML12 cells (**B**). Cells were incubated for 24 h with increasing doses of ethanol (50 - 100 mM) in medium containing 2% FBS.

C-D. Representative immunoblots and densitometric quantification for cleaved caspase-3 in primary mouse hepatocytes exposed to ethanol. Cells were incubated for 24 h without or with ethanol (50 - 100 mM) in DMEM containing 2% FBS.

E-F. The effect of alcohol exposure on cleaved caspase-3 was mimicked by overexpression of SRPK2 in primary mouse hepatocytes. Cells were transduced for 24 h with or without adenoviral vectors expressing SRPK2 or control GFP in DMEM containing 2% FBS.

G-H. Real-time qRT-PCR analysis showed that mRNA levels of CXCL1 were increased in primary hepatocytes exposed to ethanol (100 mM) or in primary hepatocytes overexpressing SRPK2.

The data are presented as the mean ± S.E.M., n=3, *P<0.05 between two groups.

Fig. S3

Li G, et al.

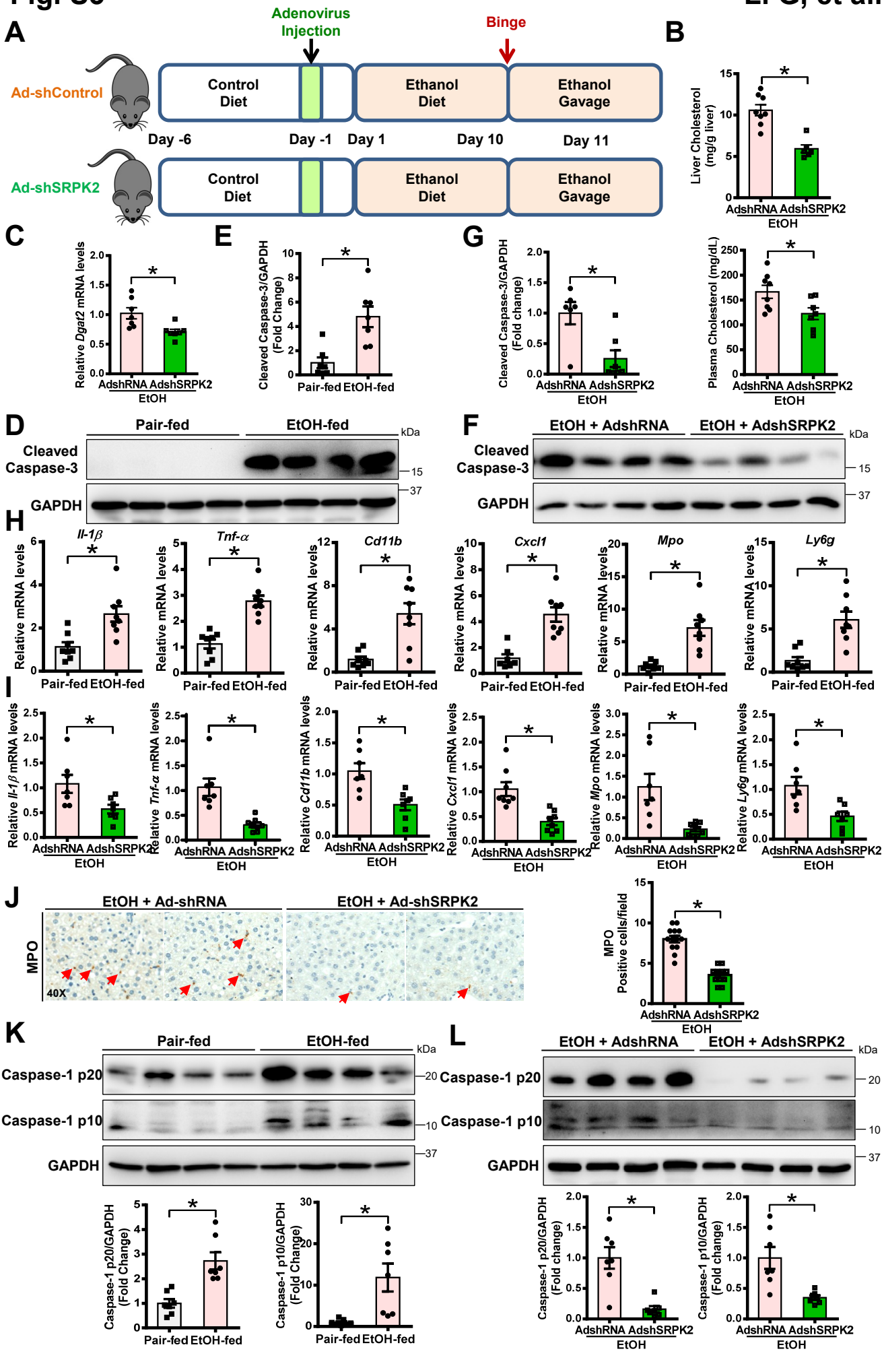

Fig. S3. Adenovirus-mediated knockdown of SRPK2 ameliorates chronic-binge alcohol feeding-induced hepatic fatty acid synthesis and steatosis in mice, related to Fig. 3.

A. The schematic illustration of a mouse model of ALD and adenovirus injection time. Adenovirus-mediated short hairpin RNA (shRNA) targeting the mouse SRPK2 gene (AdshSRPK2) or adenovirus encoding shRNA control (AdshRNA) were delivered into mice via tail vein injection. After that, adenovirus mice were subjected to a Lieber-DeCarli alcohol liquid diet for 10 days, plus one binge of alcohol at the end of experiments. The mice were sacrificed 9 hours post-binge.

B. Hepatic and plasma cholesterol levels in alcohol-fed mice that were injected with either AdshRNA control or AdshSRPK2.

C. Real-time qRT-PCR analysis of mRNA levels of *Dgat2* in livers of alcohol-fed mice that were injected with either AdshRNA control or AdshSRPK2.

D-E. Representative immunoblots and densitometric quantification for cleaved caspase-3 in pair-fed and ethanol-fed mice.

F-G. Immunoblots and densitometric quantification for cleaved caspase-3. Chronic-binge alcohol feeding-induced cell apoptosis was attenuated in mice upon SRPK2 knockdown.

H. Real-time qRT-PCR analysis of pro-inflammatory markers and cytokines, such as IL-1β and TNF-α, and the macrophage marker Cd11b, as well as the neutrophil chemokine CXCL1 and neutrophil markers, such as MPO, and Ly6g, in pair-fed and alcohol-fed mice.

I. Real-time qRT-PCR analysis showed that the alcohol-induced inflammatory response was attenuated in mice upon SRPK2 knockdown.

J. Immunohistochemistry for the neutrophil marker MPO and the number of MPO^+ cells per field in mice were shown. Notably, following alcohol feeding, positive staining for MPO^+ neutrophils (red arrows) was reduced in mice upon SRPK2 knockdown.

K-L. Immunoblots and densitometric quantification for p10 and p20 fragments of caspase-1. Alcohol-induced cleavage and activity of caspase-1 were attenuated upon SRPK2 knockdown.

The data are presented as the mean ± S.E.M., n=6-8 per group. *P<0.05 between two groups.

Images were acquired using 40X objectives.

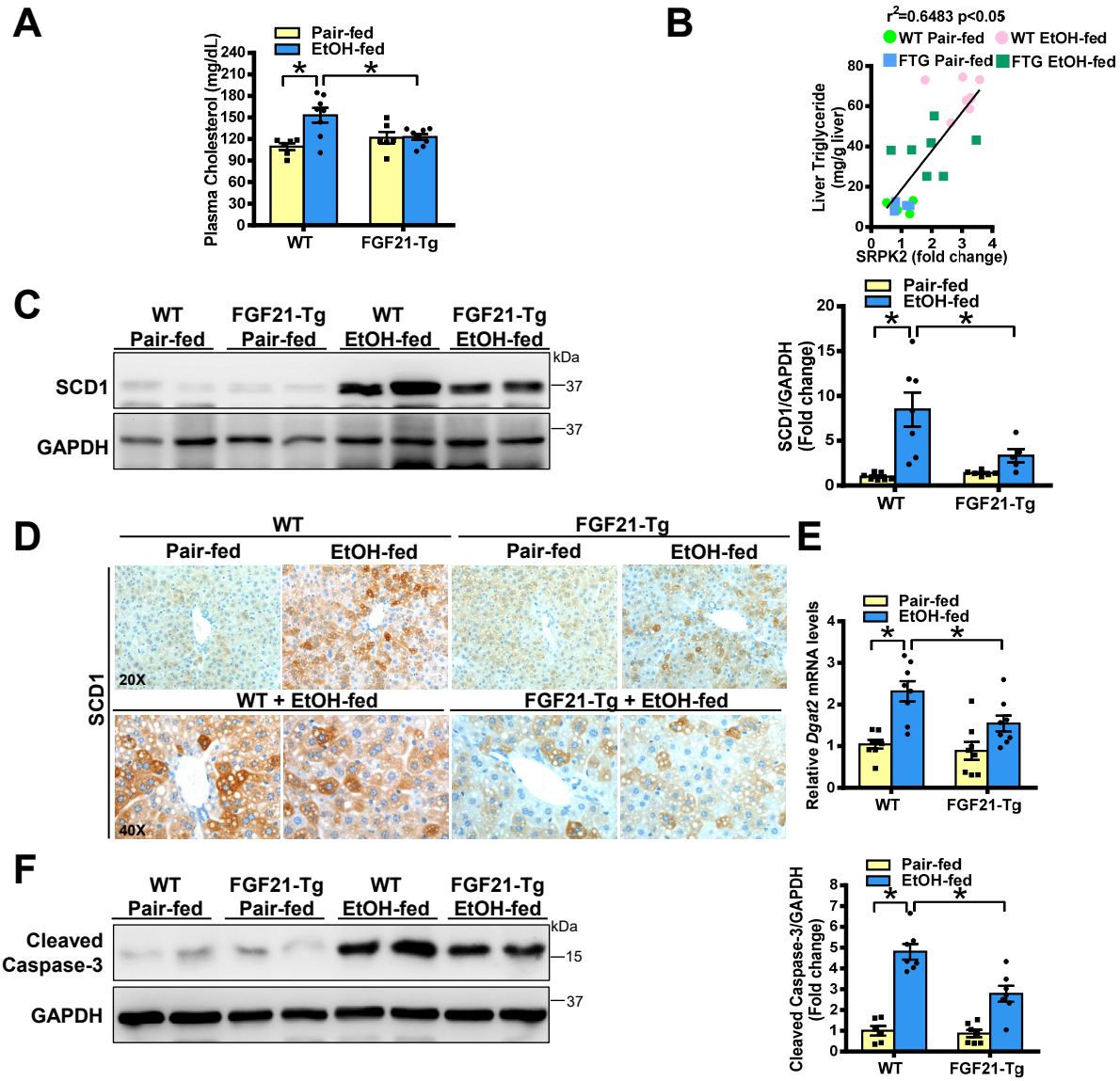

Fig. S4. Overexpression of FGF21 in transgenic mice suppresses alcohol-mediated induction of SRPK2 and protects against ALD, related to Fig. 5.

A. WT mice and FGF21-Tg mice were subjected to a Lieber-DeCarli alcohol liquid diet for 10 days, followed by one binge alcohol feeding at the end of experiments, while the control group received a pair-fed control liquid diet. All mice were sacrificed 9 hours post-binge. Plasma cholesterol levels in WT and FGF21-Tg mice.

B. Correlation between SRPK2 protein levels and liver triglyceride concentrations in WT and FGF21-Tg mice fed either a control or alcohol diet.

C. Immunoblots and densitometric quantification for SCD1.

D. Immunohistochemistry staining for SCD1. Notably, upon chronic-binge ethanol feeding, the number and distribution of SCD1^{+} hepatocytes were reduced in FGF21-Tg mice.

E. Real-time qRT-PCR analysis of mRNA levels of the lipogenic gene DGAT2 in the livers of WT and FGF21-Tg mice after chronic-binge alcohol feeding.

F. Immunoblots and densitometric quantification for cleaved caspase-3.

The data are presented as the mean ± S.E.M., n=6-8 per group. *P<0.05 between two groups. Images were acquired using 20X or 40X objectives.

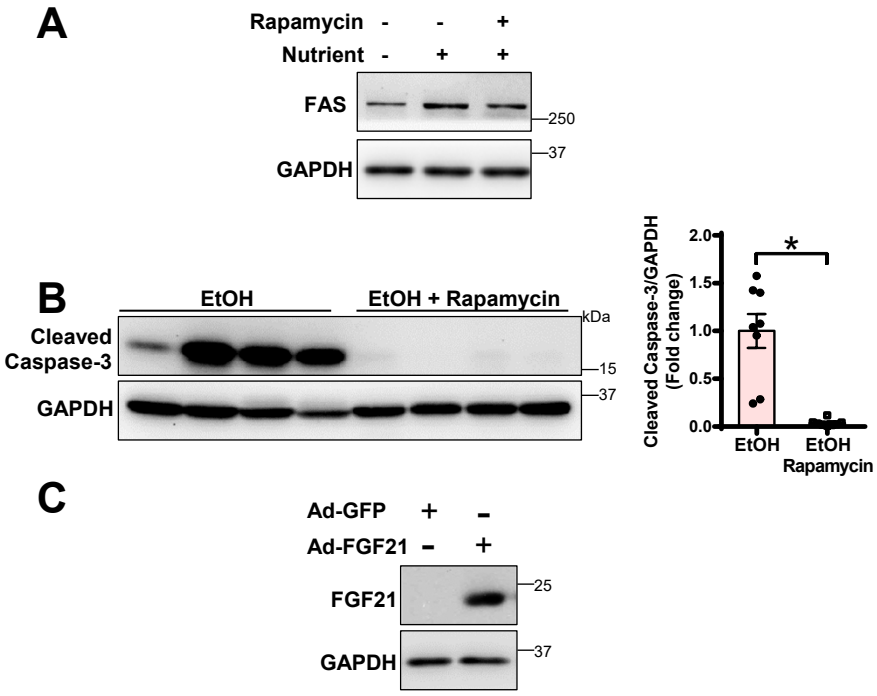

Fig. S5. FGF21 overexpression mimics the inhibitory effect of rapamycin on alcohol-induced accumulation of SRPK2 protein in hepatocytes and *in vivo,* related to Fig. 5.

A. mTORC1 inhibition by rapamycin treatment decreased FAS expression in AML-12 hepatocytes under conditions of nutrient-stimulated activation of mTORC1. AML12 cells were cultured for 24 h in medium containing 2% fetal bovine serum (FBS) or in medium containing 10% FBS (Nutrient-rich condition) in the absence or presence of rapamycin (20 nM). **B**. Immunoblots and densitometric quantification for cleaved caspase-3. Chronic-binge alcohol feeding-induced cell apoptosis was attenuated in mice upon rapamycin treatment.

The data are presented as the mean ± S.E.M., n=6-8 per group. *P<0.05 between two groups.

C. Immunoblotting analysis confirmed adenoviral overexpression of FGF21 in cultured HepG2 cells.

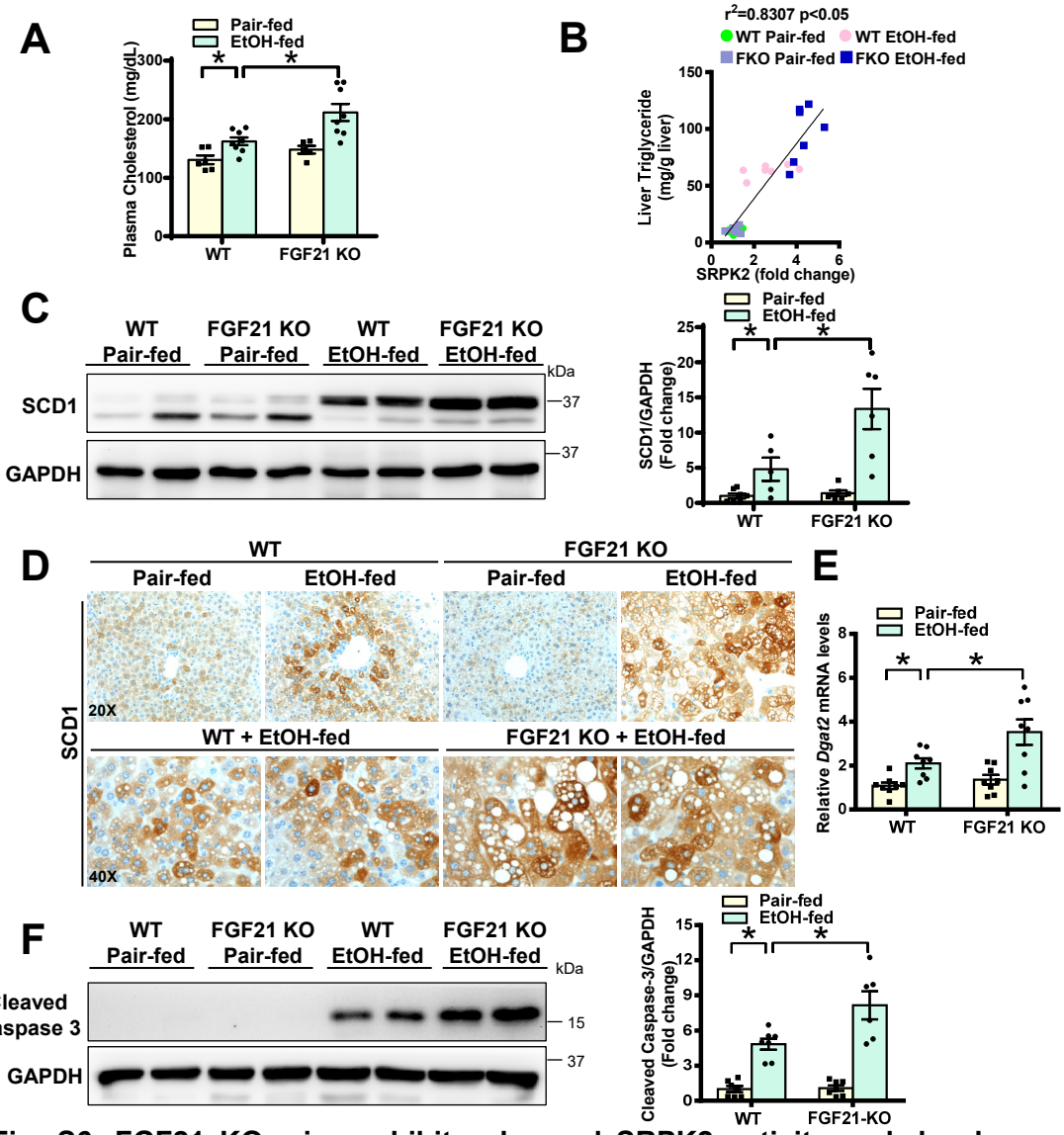

Fig. S6. FGF21 KO mice exhibit enhanced SRPK2 activity and develop more severe ALD pathologies, related to Fig. 6.

A. WT and FGF21 knockout (FGF21 KO) mice were subjected to a Lieber-DeCarli alcohol liquid diet for 10 days, followed by one binge alcohol feeding at the end of experiments, while the control group received a pair-fed control liquid diet. All mice were sacrificed 9 hours post-binge. Plasma cholesterol levels in WT and FGF21 KO mice that were fed either control or alcohol diets.

B. Correlation between hepatic SRPK2 levels and triglyceride concentrations in WT and FGF21 KO mice.

C. Immunoblots and densitometric quantification for SCD1.

D. Immunohistochemistry staining for SCD1. Upon chronic-binge ethanol feeding, positive staining for SCD1 was visualized mainly in hepatocytes of WT mice, but the distribution of SCD^{+} hepatocytes was higher in FGF21 KO mice than in WT mice.

E. Real-time qRT-PCR analysis of mRNA levels of the lipogenic gene DGAT2 in the livers of WT and FGF21 KO mice after chronic-binge alcohol feeding.

F. Immunoblots and densitometric quantification for cleaved caspase-3.

The data are presented as the mean ± S.E.M., n=6-8 per group. *P<0.05 between two groups. Images were acquired using 20X or 40X objectives.

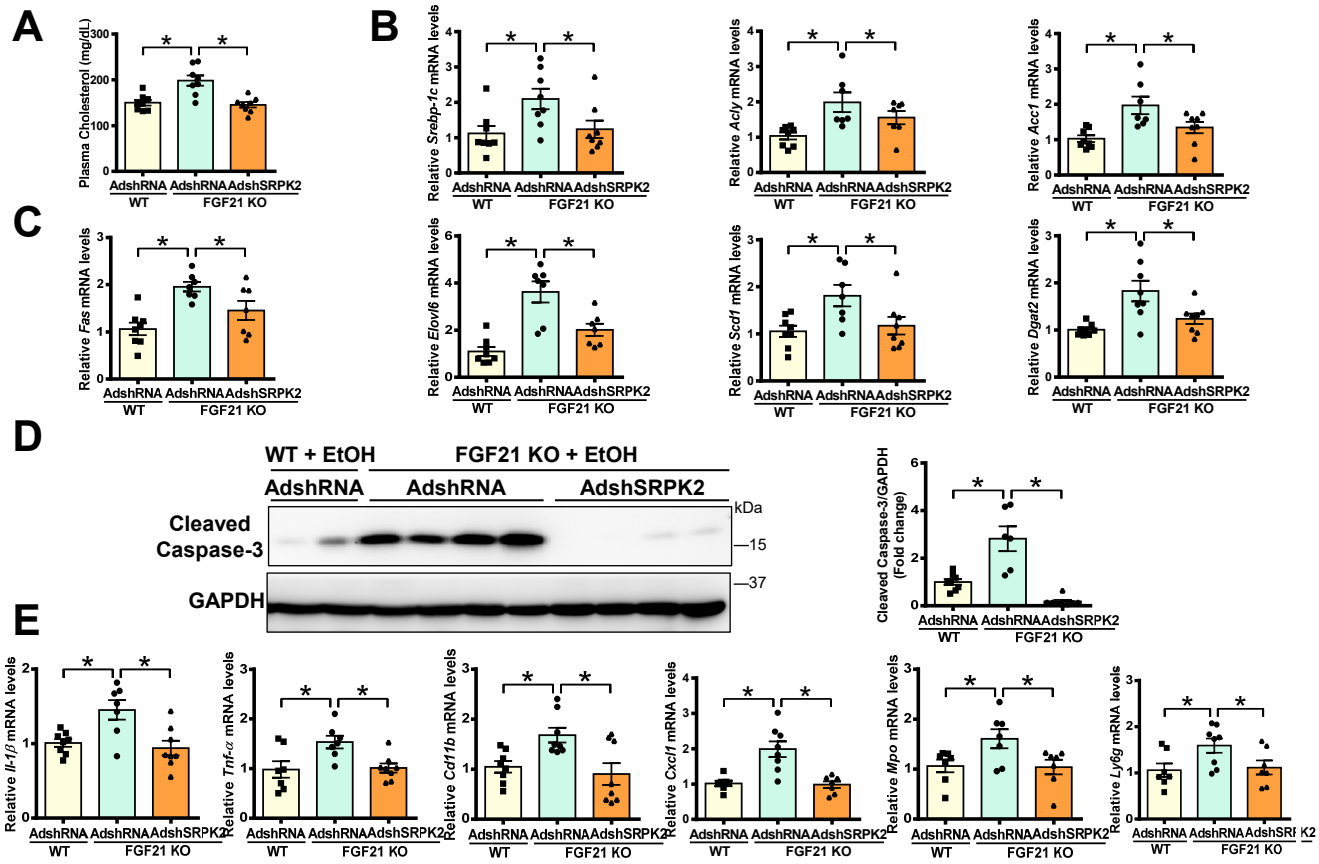

Fig. S7. Silencing hepatic SRPK2 rescues aberrant regulation of lipid metabolism and alleviates ALD pathologies in FGF21 KO mice, related to Fig. 7.

A. Either AdshSRPK2 or AdshRNA control was delivered into WT or FGF21 KO mice via tail vein injection. After that, adenovirus-injected mice were subjected to a Lieber-DeCarli alcohol liquid diet for 10 days plus one time of alcohol binge feeding at the end of experiments. The mice were sacrificed 9 hours post-binge. The elevation of plasma cholesterol levels in ethanol-fed FGF21 KO mice was lowered by silencing hepatic SRPK2.

B-C. Real-time qRT-PCR analysis of mRNA levels of SREBP-1 and its target genes**.**

D. Immunoblots and densitometric quantification for cleaved caspase-3.

E. Real-time qRT-PCR analysis of mRNA levels of pro-inflammatory mediators.

The data are presented as the mean ± S.E.M., n=6-8 per group. *P<0.05 between two groups.

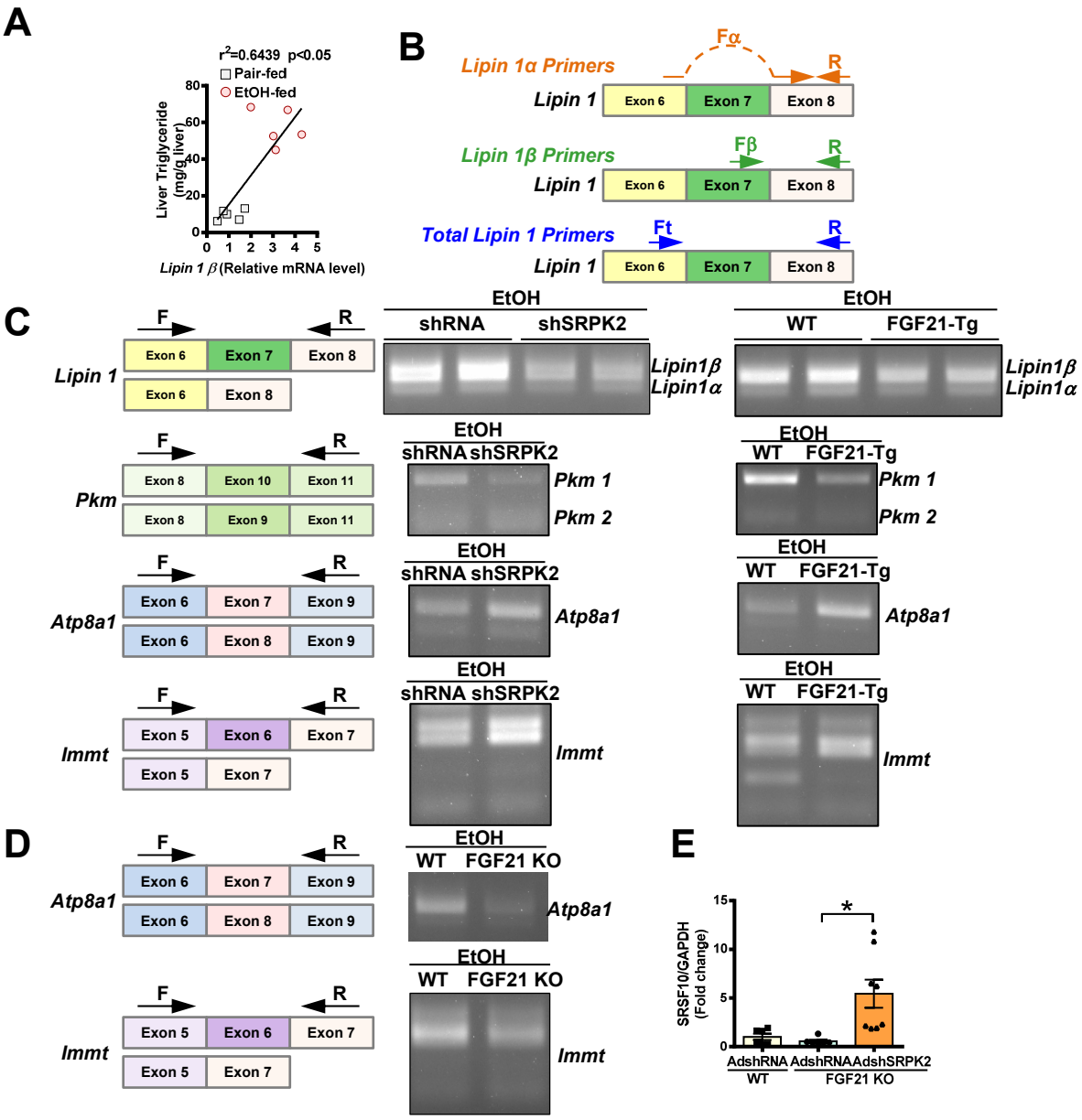

Fig. S8. Manipulation of SRPK2 and FGF21 in mice modulates dysregulation of SRSF10-mediated pre-mRNA splicing associated with ALD, related to Fig. 8.

A. Correlation between induction of lipin 1β and elevation of liver triglyceride levels in mice.

B. Schematic illustration shows the specific primers designed to amplify different lipin 1 spliced isoforms. Specifically, to detect and amplify the transcript of lipin 1α spliced isoform that lacks exon 7, the forward primer spans the junction between the upstream exon 6 and downstream exon 8, in the absence of any exon 7 sequence, while the reverse primer is located in exon 8. To detect the lipin 1β spliced isoform that includes exon 7, the forward primer is located in exon 7, while the reverse primer is the same as for lipin 1α. To assess mRNA levels of total lipin 1, the forward primer is located in exon 6, while the reverse primer is the same as for lipin 1α. Real-time qRT-PCR analysis was conducted using these primers to assess mRNA levels of different spliced isoforms of the lipin 1 gene, as well as total lipin 1 mRNA levels.

C. The *in vivo* effect of silencing SRPK2 and overexpressing FGF21 on SRSF10 splicing function. RT-PCR analysis of alternative splicing of SRSF10 target genes, such as lipin 1, PKM, Atg8a1, and Immt. The schematic illustration shows specific primers that localize pre-mRNA sequences flanking the spliced exon-exon junction. RT-PCR analysis was performed using these primers to detect and amplify spliced products for target genes of SRSF10.

D. RT-PCR analysis of alternative splicing of Atp8a1 and Immt in WT and FGF21 KO mice.

E. Densitometric quantification for SRSF10. After alcohol administration, hepatic SRSF10 was downregulated in AdshRNA control-injected FGF21 KO mice, and this impairment was rescued by silencing SRPK2.